

Modeling of discharges generated by electron beams in dense gases: Fountain and thunderstorm regimes

S. O. Macheret, M. N. Shneider, and R. B. Miles
*Princeton University, Department of Mechanical and Aerospace Engineering,
D-414 Engineering Quadrangle, Princeton, New Jersey 08544*

(Received 1 September 2000; accepted 16 February 2001)

In this paper we present an analysis of the predicted dynamics of plasmas generated in air and other gases by injecting beams of high-energy electrons. Two distinct regimes are found, differing in the way that the excess negative charge brought in by the ionizing electron beam is removed. In the first regime, called a fountain, the charge is removed by the back current of plasma electrons toward the injection foil. In the second, called a thunderstorm, a substantial cloud of negative charge accumulates, and the increased electric field near the cloud causes a streamer to strike between the cloud and a positive or grounded electrode, or between two clouds created by two different beams. A quantitative analysis, including electron beam propagation, electrodynamics, charge particle kinetics, and a simplified heat balance, is performed in a one-dimensional approximation. © 2001 American Institute of Physics. [DOI: 10.1063/1.1363666]

I. INTRODUCTION

When beams of energetic electrons propagate into a gas, they lose their energy by ionizing and exciting the gas molecules, with 30–50% of the beam energy spent directly on ionization. Use of electron beams as an efficient ionization source to stabilize electric discharges is well known and widely used, in particular, in electric discharge lasers.¹

The propagation of an electron beam injected into a background, initially neutral, gas is a complex and multiparametric problem.² Considerable experimental and theoretical work has been done on the interaction of electron beams with gases, where beam-induced ionization, return current, and charge neutralization strongly affect the propagation of the beam.^{2–5} Theoretical work on beam–gas interactions performed to date can be divided into three principal categories.

The first category, represented, e.g., by Ref. 3, addresses relativistic (MeV-class) high-current (kiloamperes) pulsed beams. Because of the high currents and fast (nanosecond) transients, self-induced magnetic and electromagnetic effects, coupled with plasma generation, are of primary importance. However, the beam is assumed to be unaffected by its passage through the gas. This assumption is valid when the beam relaxation length is very large, which is the case for an MeV-class beam propagating into a low-to-moderate pressure gas, so that the beam energy is almost constant within the spatial region of interest.

The second category of papers addresses diffuse electric discharges supported by electron beams with applications to high-power lasers and fast switches,^{1,6} or to plasma reflectors of electromagnetic waves.^{7–10} The main requirement for the electron beam (injected from the cathode to the anode) in those discharges is to provide a uniform ionization throughout the volume. For this, the beam relaxation length should exceed the interelectrode gap, $l_r > L$. In this situation, varia-

tion of beam energy and current along its path is again quite small, simplifying theoretical analysis.

In the third group of papers on electron beam interactions with gases details of the energy distribution of electrons in beam-produced plasmas are addressed.^{11–13} Because of complexity of the problem, those analyses are zero-dimensional, i.e., uncoupled from beam propagation and beam-produced ionization.

In this paper, we consider beams with initial energy of between 1 keV to a few hundred keV and a current density of 1–100 mA/cm² propagating into a gas at a pressure from about 1 Torr to several atmospheres. We will be interested in a situation where the beam loses its energy and ionizes the gas far from the walls, and where the tip of the beam-produced plasma does not reach the anode. The low beam current allows us to neglect self-induced magnetic and electromagnetic effects. On the other hand, the relatively low beam energy and high gas density result in a relatively short beam penetration length, from a few centimeters to perhaps a few meters. Over this length, the energy of beam electrons varies quite significantly, so that the beam propagation is coupled with plasma generation, motion of charged particles, gas heating, and spatio-temporal evolution of the electric field. In this paper, we develop a model for these coupled phenomena.

One of the main issues in the case where a beam loses its energy before reaching any wall or an anode is the mechanism of charge neutralization. When injected into a gas through a cathode toward an anode, an electron beam generates both a plasma and a cloud of negative space charge. As a result, the electric potential inside the gap becomes lower than the potential of either of the two electrodes. If the pre-existing anode voltage is high, and the beam stops close to the anode without actually touching it, then the electron beam can quickly bring negative potential close to the anode,

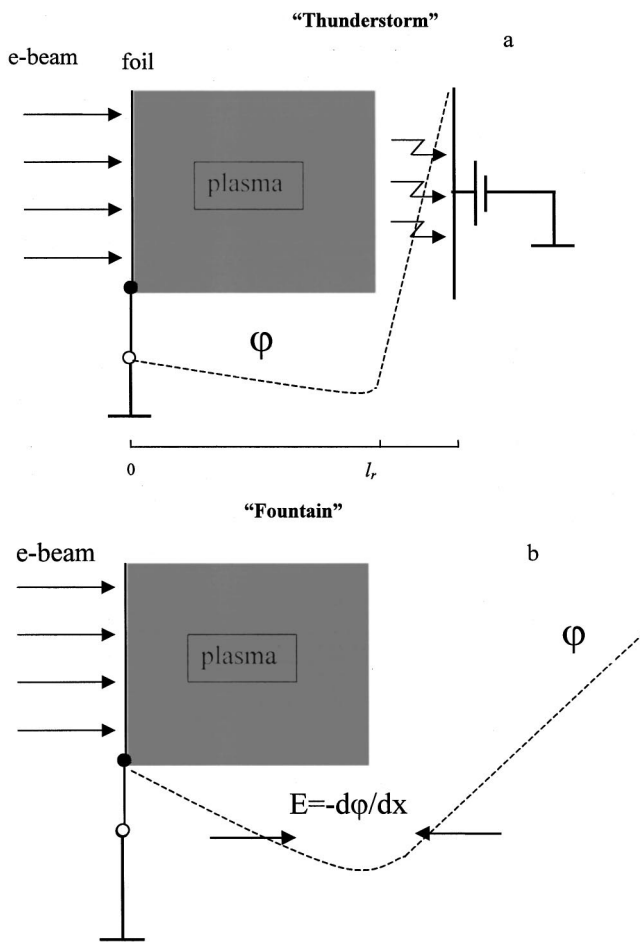


FIG. 1. Schematic of fountain and thunderstorm regimes. The electron beam is injected through into the gas from left to right. ϕ is the electric potential and E is the field.

and the cloud will quickly accumulate such a charge that electric field near it can exceed the breakdown threshold of the ambient gas, creating either a streamer or Townsend breakdown between the cloud and the positively biased anode plate [Fig. 1(a)].

The sparks, or streamers, can be generated at a high repetition rate by using a repetitive-pulse electron beam. With multiple electron beams, sparks will occur between the clouds as well as between each cloud and the earth (grounded plate). Since this process of removal of the excess negative charge is similar to lightning between thunderclouds and the earth and between the thunderclouds, we shall call the process a thunderstorm.

One can also envisage a very different mechanism of charge neutralization: a quasistationary discharge between the virtual cathode at the tip of the beam-produced cloud and the metallic foil through which the beam is injected into the gas. In such a fountain discharge, the return current of plasma electrons will balance the forward current of high-energy beam electrons. In principle, to sustain such a discharge at steady state, the second electrode (the anode to which the voltage is applied) is not necessary. Thus, a quasisteady-state, stable, high-pressure discharge could be created with a single electrode [Fig. 1(b)]. In its structure and

properties, electron beam-sustained single-electrode discharge should be similar to conventional glow discharge (except that the electron temperature in beam-produced plasmas could be very low—see Secs. II and III). The beam injection foil acts as an anode, and the tip of the cloud of injected negative charge serves as a virtual cathode for the fountain discharge. Of course, the cathode of the electron gun where the beam originates is the real cathode for the system as a whole.

II. ONE-DIMENSIONAL MODELING OF ELECTRON BEAM INJECTION, DISTORTION OF ELECTRIC FIELD, AND PLASMA GENERATION

To analyze the dynamics of beam-generated plasmas, let us consider a 1D model of a non-self-sustained high-pressure gas discharge, supported by an electron beam whose relaxation length, l_r , is shorter than the interelectrode gap L (Fig. 1). The foil through which the beam is injected is considered as one of the electrodes. In reality, a metallic holder electrically insulated from the foil by dielectric seals can have a potential applied to it and serve as an electrode. In the simple 1D model, though, the holder-electrode is indistinguishable from the foil-electrode.

Of course, 1D modeling could be quite restrictive. Even if the original electron beam is unidirectional and monoenergetic, scattering inside the foil and in the dense gas could make the problem three-dimensional. The problem would be close to one-dimensional one if the injection foil is very thin, or if a differentially pumped port is used instead of a foil for beam injection. Additionally, a strong magnetic field could be used to inhibit beam and plasma expansion. Thus, the following 1D analysis could be viewed as a first approximation in the case of beam injection through a thin foil or a differentially pumped port, with a strong guiding magnetic field.

There are two groups of electrons in the system: plasma electrons, with the number density n_e , and beam electrons, with the number density n_b . The latter group is described by a simplified kinetic equation in the so-called forward approximation.¹⁴ The approximation takes into account only inelastic electron-molecule collisions that are assumed not to change the direction of electron motion. This approximation is well justified in our case, since for the most relevant, ionizing, high-energy part of the degradation spectrum of the beam, inelastic cross sections considerably exceed the momentum-transfer cross section: $\sigma_k^n(\epsilon) \gg \sigma_m(\epsilon)$, when $\epsilon > 1000$ eV. The subscript k denotes various chemical constituents of the gas. Thus, the contribution of elastic collisions is small and we shall neglect them, assuming that all electrons move only in the direction normal to the foil (x -direction) at a speed of $v = (2\epsilon/m)^{1/2}$. (This expression for the velocity is valid, of course, only for nonrelativistic electrons.) Then the spectral density of the electron flux, $\Gamma(\epsilon, x)$ is determined directly by the coordinate-dependent electron energy distribution function $n(\epsilon, x)$: $\Gamma(\epsilon, x) = vn(\epsilon, x)$. Making the transformation from 1D velocity distribution function ($v_x \equiv v$) to the energy distribution function, with $f(v, x)dv = n(\epsilon, x)d\epsilon$, we obtain the equation¹⁴

$$\frac{\partial \Gamma}{\partial x} - eE(x,t) \frac{\partial \Gamma}{\partial \epsilon} = Q(\Gamma) = - \sum_{n,k} N_k \Gamma(x, \epsilon) \sigma_k^n(\epsilon) + \sum_{n,k} N_k \Gamma(x, \epsilon + I_k^n) \sigma_k^n(\epsilon + I_k^n). \quad (1)$$

Here, excitation of the n -th quantum state of the molecule of the k -th component, requiring electron energy I_k^n , and electron-impact ionization, requiring, in the first approximation, energy equal to the ionization potential I_k , contribute to the inelastic collision term Q . $\sigma_k^n(\epsilon)$ are the excitation and ionization (in the case of ionization, superscript $n=i$) cross sections, and N_k is the number density of the k -th chemical component of the gas.

Total beam electron number density at a given location is

$$n_b(x) = \int_{\min I_k}^{\infty} \frac{\Gamma(x, \epsilon) d\epsilon}{\sqrt{2\epsilon/m}}. \quad (2)$$

The net flux, that is, the net number of beam electrons passing through unit area per unit time in the x direction, is

$$\Gamma_b(x) = \int_{\min I_k}^{\infty} \Gamma(x, \epsilon) d\epsilon. \quad (3)$$

The local ionization rate, that is, the number of ionization events in 1 cm³ per 1 second at a given location x , is

$$q(x) = \sum_k N_k \int_{I_k}^{\infty} \Gamma(x, \epsilon) \sigma_k^i(\epsilon) d\epsilon. \quad (4)$$

In an electron-impact ionization event, a part of energy ϵ of the impinging electron goes into production of the secondary electron, and a part goes into kinetic energy ϵ' of that electron. Details of the energy spectrum of secondary electrons, described by differential ionization cross sections, and the effect of that spectrum on electron energy distribution, excitation, and ionization rates, have been studied elsewhere.^{11–13,15,16} The nascent spectrum of secondary electrons has a sharp maximum at about 5 eV, which is substantially lower than the ionization energy, and the probability for the secondary electron to immediately ionize a molecule is quite small.^{11–13,15,16} At pressures of hundreds of Torr, secondary electrons will rapidly lose the memory of their nascent distribution and form the energy distribution function corresponding to the local value of E/N .^{11–13,15,16} Because of this, details of the nascent spectrum were found to be unimportant,^{11–13,15} and simply assuming that new electrons are produced with either zero energy or with a mean energy corresponding to the local plasma electron temperature, $T_e(x)$, turned out to yield reasonably accurate energy distribution functions and kinetic rates.^{11–13,15,16} The contribution of secondary (plasma) electrons to the total ionization rate is, therefore, determined by the electron temperature, or, more exactly, by the value E/N [see Eqs. (6)–(8) below].

One of the well-known parameters of electron beam interaction with gases is the so-called ionization cost, Y_k , that is, the mean energy of production of an electron-ion pair in beam electron collisions with molecules of the k -th compo-

nent. At primary electron energies above a few hundred eV, Y_k is virtually independent of the beam energy, and is determined by the gas composition only. For example, in air, pure nitrogen, and oxygen, $Y_k=34$ eV, 35 eV, and 30.9 eV, respectively.¹ Therefore, in the inelastic collision integral Q for fast electrons, the term corresponding to the source of electrons of energy ϵ due to ionization can be written approximately as

$$\sum_k N_k \Gamma(x, \epsilon + Y_k) \sigma_k^i(\epsilon + Y_k), \quad \epsilon + Y_k \leq \epsilon_b,$$

where ϵ_b is the beam electron energy. For simplicity, we shall assume that the injected beam is monoenergetic, so that the boundary condition for the beam is

$$\Gamma(0, \epsilon) = (|j_b|/e) \delta(\epsilon - \epsilon_b), \quad (5)$$

where j_b is the electron beam current density, and ϵ_b is the energy of the injected electrons. Obviously, by modifying this boundary condition, effects of injection of a beam that is not monoenergetic can be easily accounted for.

Note that the forward approximation for the kinetic equation was used here only to shorten the computations. There are no principal difficulties, except making computations longer, in using a more complete forward-back approximation accounting for backscattering and elastic collisions. Importantly, integral parameters of the beam-gas interaction, such as the relaxation length, $l_r = l_r(\epsilon_b, N(x))$, the total rate of production of electron-ion pairs, $\text{Int}_1 = \int q dx = \text{Int}_1[\epsilon_b, j_b, N(x)]$, and the total gas heating rate, $\text{Int}_2 = \int Q_b dx = \text{Int}_2[\epsilon_b, j_b, N(x)]$, are independent of the type of kinetic equation used.

An example of the computed relaxation of a beam with an energy $\epsilon_b = 15$ keV injected into a room air at $p = 1$ atm $T(x) = 300$ K = const is shown in Fig. 2.

To describe the beam-generated plasma and the discharge, we used the following set of continuity equations for plasma electrons, n_e , and positive, n_+ , and negative, n_- , ions, plus the Poisson equation for the potential:

$$\frac{\partial n_e}{\partial t} + \frac{\partial \Gamma_e}{\partial x} = q + \alpha |\Gamma_e| + k_d N n_- - \nu_a n_e - \beta n_e n_+ - \frac{\delta n_b}{\delta t},$$

$$\Gamma_e = -\mu_e n_e E - D_e \frac{\partial n_e}{\partial x} - k_T D_e \frac{n_e}{T_e} \frac{dT_e}{dx}, \quad (6)$$

$$\frac{\partial n_+}{\partial t} + \frac{\partial \Gamma_+}{\partial x} = q + \alpha |\Gamma_e| - \beta_{ii} n_- n_+ - \beta n_e n_+,$$

$$\Gamma_+ = \mu_+ n_+ E - D_+ \frac{\partial n_+}{\partial x}, \quad (7)$$

$$\frac{\partial n_-}{\partial t} + \frac{\partial \Gamma_-}{\partial x} = -k_d N n_- + \nu_a n_e - \beta_{ii} n_- n_+,$$

$$\Gamma_- = -\mu_- n_- E - D_- \frac{\partial n_-}{\partial x}, \quad (8)$$

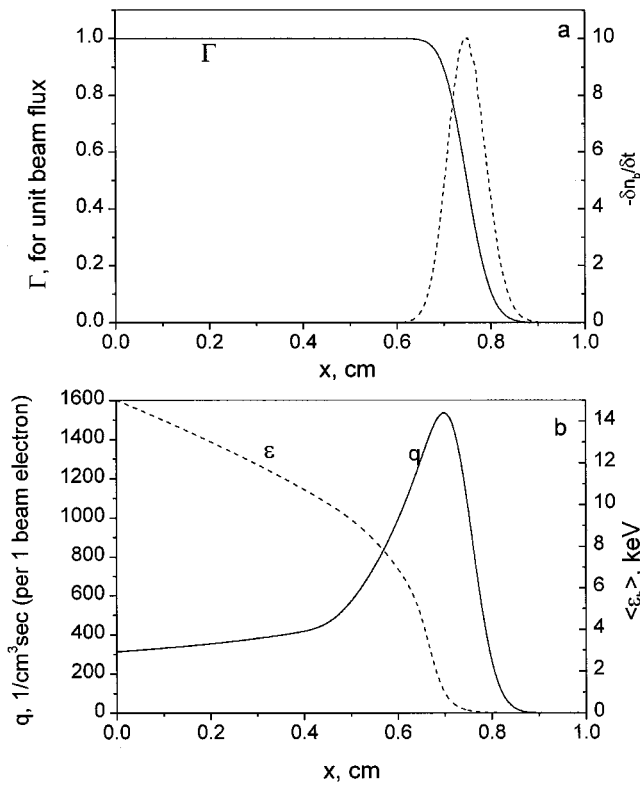


FIG. 2. Computed steady-state relaxation of an electron beam injected parallel to the x coordinate at $x=0$ into room-temperature air at $p=1$ atm. Beam energy is $\epsilon_b=15$ keV. (a) Flux of beam electrons, Γ , and beam thermalization rate, $\delta n_b / \delta t = d\Gamma_b / dx$; (b) mean electron energy, $\langle \epsilon \rangle$, and ionization rate, q .

$$\frac{\partial^2 \varphi}{\partial x^2} = -\frac{e}{\epsilon_0} (n_+ - n_e - n_- - n_b), \quad E = -\frac{\partial \varphi}{\partial x}. \quad (9)$$

In Eqs. (6)–(9), q is the beam-induced ionization rate determined by Eq. (4), and $\alpha = \alpha(E/N)$ is the first Townsend ionization coefficient¹⁷ that describes avalanching, i.e., further ionization of the background gas by secondary (plasma) electrons. An additional source term due to thermalization of beam electrons, $-\delta n_b / \delta t = -d\Gamma_b / dx$, is also included in Eq. (6). To correctly describe charge transport in regions with a very low electric field, the expressions for the fluxes Γ_e , Γ_+ , and Γ_- include both drift (with mobilities μ_e , μ_+ , and μ_-) and diffusion (with electron, positive ion, and negative ion diffusion coefficients D_e , D_+ , and D_- , respectively) terms, as in modeling the negative glow of conventional glow discharges.¹⁸ Electron temperature and mobility were taken as functions of the local value of E/N , $T_e(E/N)$, and $\mu_e(E/N)$. These functions were taken from the tabulated results of a direct solution of the Boltzmann kinetic equation for air.¹⁹ At very low E/N , $E/N < 1$ Td, where the approximation for μ_e given in Ref. 19 is not valid, we used the approximation $\mu_e(T_e) = \tilde{\mu}_e(\tilde{T}_e / T_e)^{0.5}$, where $\tilde{\mu}_e$, \tilde{T}_e are the values at $E/N=1$ Td. The last approximation follows from the definition of electron mobility and the approximation of an energy-independent mean free path:¹⁷ $\mu_e = e/m\nu_m \approx el_m/mv(T_e)$, where ν_m is the momentum-transfer collision frequency, and l_m is the mean free path of

electrons. The approximate values of mobility for both positive and negative ions were taken from Ref. 17: $\mu_{+,-} = 1.75 \times 10^3 / (p \cdot 300/T)$ $\text{cm}^2/\text{V}\cdot\text{s}$, where pressure p is in Torr. The diffusion coefficients were determined from the respective mobilities using the Einstein relation: $D_e = \mu_e T_e$; $D_{+,-} = \mu_{+,-} T$.

The value of electron temperature at very low E/N , $E/N \leq 1$ Td, where the approximation for μ_e given in Ref. 19 is not valid, is expected to be quite low, 0.1 eV or lower, i.e., within a factor of 2 of gas temperature. This follows from the electron energy distributions in beam-produced plasmas without an electric field.^{11–13,15,16} Note also that the plasma in the electron beam-generated cloud should have properties close to those of negative glow plasmas of conventional glow discharges. Electrons in negative glow plasmas are known to have low temperatures, down to the neutral gas temperature.²⁰ Therefore, in our computations, we assumed that $T_e(x,t) = 2T(x,t)$ whenever E/N is of the order of 1 Td or lower.

We used standard boundary conditions at the electrodes. These conditions are commonly used to model gas discharges with cold cathodes. For example, at $x=0$, in the absence of negative ions ($n_- = 0$),

$$\Gamma_e = -\gamma \Gamma_+; \quad \partial n_+ / \partial x = 0, \quad \text{if } E(0,t) \leq 0, \quad (10a)$$

$$\Gamma_+ = 0; \quad \partial n_e / \partial x = 0, \quad \text{if } E(0,t) > 0, \quad (10b)$$

where γ is the effective secondary emission coefficient, that is, the average number of electrons emitted for each ion impinging on the surface.

Boundary conditions for the Poisson equation are

$$\varphi(0) = 0, \quad \varphi(L) = V. \quad (11)$$

Relaxation of an electron beam results in gas heating. This decreases the gas density, affecting beam-induced ionization rate and the beam penetration depth. To model processes coupled with the heating, principal mechanisms of heating and cooling have to be identified. Energy is added to the plasma by both the electron beam and Joule dissipation. A part of the added energy goes directly into heat, while some energy is spent on excitation of vibrational and electronic molecular states. What part of the Joule dissipation rate jE goes into vibrational and electronic excitation is determined by the value of E/N ,^{17,19} and at $E/N=1-70$ Td vibrational excitation of oxygen and nitrogen consumes about 50–90% of jE . However, in all cases computed in this paper, the rate of energy addition by the beam turned out to be more than an order of magnitude higher than the Joule dissipation rate (see below), and thus the Joule dissipation could be neglected. As to the beam energy dissipation, only about 5% of it goes into vibrational excitation of nitrogen and oxygen,^{11–13} and about 30–40% of the beam energy goes into excitation of electronic states. The electronic states can be expected to quench rapidly at high pressures (hundreds of Torr). About 10–30% of the energy released in quenching can end up in vibrational modes of molecules, thus increasing the fraction of beam energy spent on vibrational excitation to perhaps 10–15%. Some of the electronic states excited by the beam are radiative, however, a 1 cm

wide column of high-density gas is optically thick for many of those radiative transitions. As a result, most of the energy dissipated by the beam is spent on gas heating, and the rate of energy loss by the beam can be, with an accuracy of 10%–20%, considered equal to the gas heating rate. Thus, to model gas heating, we need to add to the set of equations (6)–(9) the equation of state,

$$p = R\rho T = R\rho_0 T_0 = \text{const}, \quad (12)$$

and heat balance:

$$\rho c_p \frac{dT}{dt} = q_h - \Theta, \quad (13)$$

where

$$q_h = - \frac{\partial[\Gamma_b(x) \cdot \langle \epsilon_b(x) \rangle]}{\partial x} \quad (14)$$

is the rate of gas heating by the relaxing beam,²¹

$$\langle \epsilon_b(x) \rangle = \frac{\int_{\min(I_k)}^{\infty} (\Gamma(x, \epsilon) / \sqrt{2\epsilon/m}) \epsilon d\epsilon}{\int_{\min(I_k)}^{\infty} (\Gamma(x, \epsilon) / \sqrt{2\epsilon/m}) d\epsilon} \quad (15)$$

is the mean energy of the beam electrons, and Θ is the rate of heat removal by all mechanisms (thermal diffusion, convection, etc.) combined.

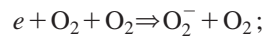
Initial conditions used in the computations were $T(x, 0) = T_0 = 300$ K; $n_e(x, 0) = n_+(x, 0) = n_-(x, 0) = 0$.

The collision cross sections necessary for the calculations of electron beam propagation and beam-induced ionization rates were taken from the literature.^{22–24} For charge particle kinetics in the plasma, the following set of processes and their rate coefficients was used. (In all the following expressions for rate coefficients, pressure p is in Torr, and temperatures T_e and T are in K.)

The electron–ion dissociative recombination rate coefficient is^{25,17} $\beta = 2 \times 10^{-7} (300/T_e)^{1/2}$, cm³/s.

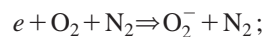
The ion–ion recombination rate coefficient (dependent on the gas density) is expressed as¹⁷ $\beta_{ii} = 1 \times 10^{-6} (0.5 + 1.5p/760) \cdot 300/T$, cm³/s.

Three-body attachment processes and their rates are²⁵



$$k_{a1} = 1.4 \times 10^{-29} \left(\frac{300}{T_e} \right) \exp\left(- \frac{600}{T} \right)$$

$$\times \exp\left(\frac{700(T_e - T)}{T_e T} \right) \text{ cm}^6/\text{s},$$



$$k_{a2} = 1.07 \times 10^{-31} \left(\frac{300}{T_e} \right)^2 \exp\left(- \frac{70}{T} \right)$$

$$\times \exp\left(\frac{1500(T_e - T)}{T_e T} \right) \text{ cm}^6/\text{s}.$$

Analysis shows that because of the substantial threshold energy for the dissociative attachment, $e + \text{O}_2 + 3.6\text{eV} \Rightarrow \text{O}$

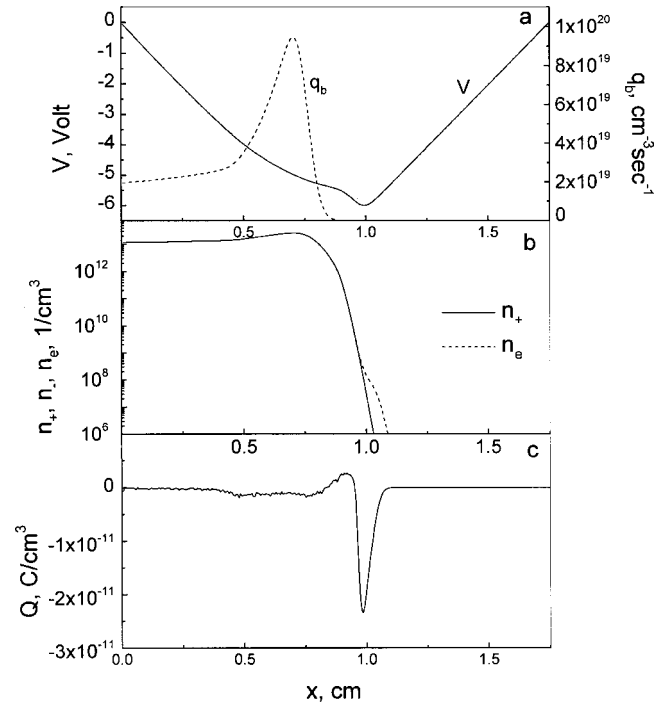
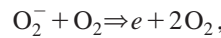


FIG. 3. Computed quasi-steady-state ($t = 10 \mu\text{s}$ from the start of beam injection) profiles of plasma parameters along the x coordinate in the fountain regime in room-temperature nitrogen at $p = 1$ atm. The electron beam current density is 10 mA/cm^2 , and the energy of beam electrons is $\epsilon_b = 15 \text{ keV}$. (a) Electric potential, V , and ionization rate, q_b ; (b) electron and ion number densities; (c) electric charge density, Q .

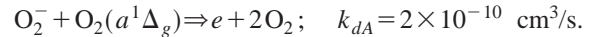
+ O^- , at very low E/N typical for the plasmas that we consider, the dissociative attachment can be neglected.

Thermal detachment and its rate coefficient are²⁶



$$k_{d\text{O}_2} = 8.6 \times 10^{-10} \exp\left(- \frac{6030}{T} \right) \left[1 - \exp\left(- \frac{1570}{T} \right) \right], \text{ cm}^3/\text{s}.$$

If active particles, such as electronically excited or radical species, are present in the plasma in large numbers, they can cause electron detachment from negative ions, e.g.,



Because of these detachment processes, the detachment frequency can be generally written as $\nu_d = k_{d\text{O}_2} N_{\text{O}_2} + k_{dA} N_A$, where N_{O_2} and N_A are the number densities of oxygen molecules and active (excited or radical) particles, respectively.

III. RESULTS OF THE MODELING

A. Fountain

A comparison of the computational results for cold [$T(x) = 300 \text{ K} = \text{const}$] nitrogen (Figs. 3 and 4) and air (Figs. 5, 6, and 7), with the same electron beam parameters ($j_b = 10 \text{ mA/cm}^2$, $\epsilon_b = 15 \text{ keV}$) clearly demonstrates the role of electron attachment to oxygen that generates negative ions, reducing the maximum electron density at steady state.

Despite the difference between nitrogen and air, in both cases the injection of the beam leads to the accumulation of

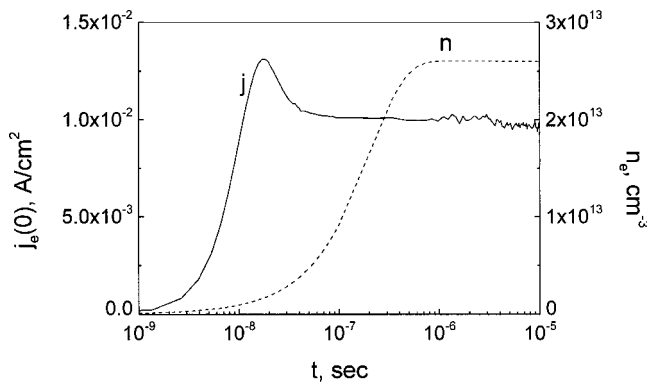


FIG. 4. Back current of plasma electrons to the foil, $j_e(0)$, and peak electron density in the plasma, n_e , versus time from the start of beam injection in the fountain regime. The gas and beam parameters are the same as in Fig. 3.

negative charge and to the growth of plasma conductivity. The process continues until a quasiequilibrium is reached: the charge that the beam brings in per unit time is fully balanced by the back flux of negative charge due to the drift of plasma electrons. The time scale of reaching the quasiequilibrium is $t \approx 0.1 \mu\text{s}$. Profiles of the power deposited by electron beam, q_h , Joule dissipation due to plasma electrons, $j_e E$, and the reduced electric field, E/N , at $t = 10 \mu\text{s}$ from the start of beam injection in the fountain regime in air initially at STP are shown in Fig. 7. As seen in Fig. 7, the electric field in the plasma is very weak, $E/N \leq 1.5 \text{ Td}$. Thus, plasma electron temperature should be close to the gas temperature, and the Joule dissipation rate is much lower than the rate of

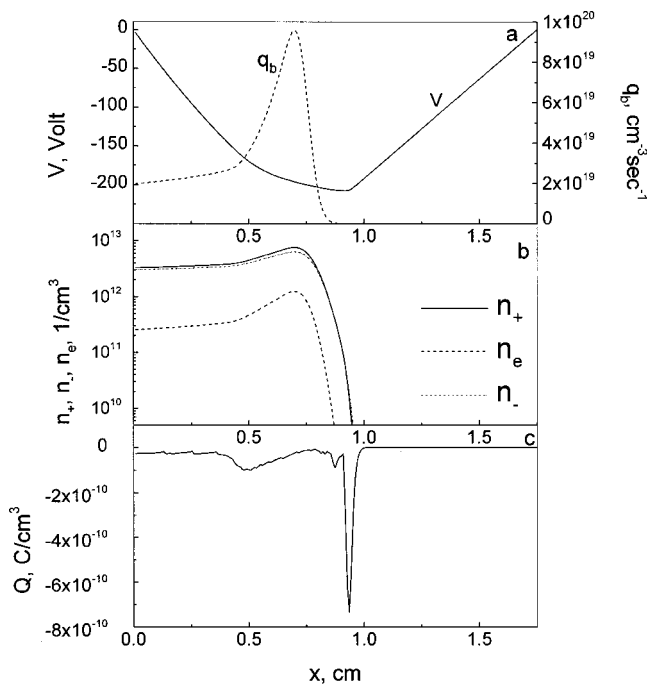


FIG. 5. The computed quasi-steady-state ($t = 10 \mu\text{s}$ from the start of beam injection) profiles of plasma parameters along the x coordinate in the fountain regime in air at STP. Electron beam current density is 10 mA/cm^2 , and the energy of beam electrons is $\epsilon_b = 15 \text{ keV}$. (a) Electric potential, V , and ionization rate, q_b ; (b) electron and ion number densities; (c) electric charge density, Q .

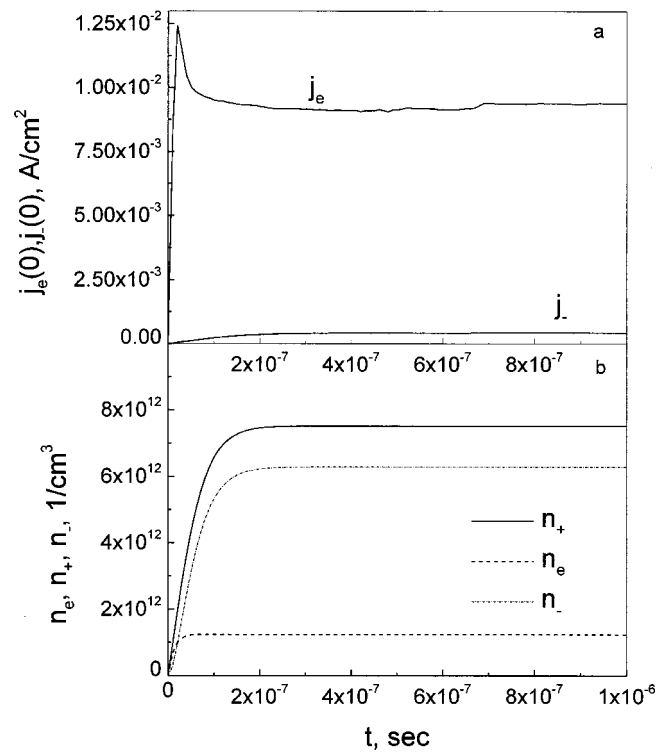


FIG. 6. Back current of plasma electrons to the foil, $j_e(0)$, and peak electron and positive and negative ion densities in the plasma, n_e , n_+ , and n_- , versus time from the start of beam injection in the fountain regime. The gas and electron beam parameters are the same as in Fig. 5.

beam energy losses. According to the data of Ref. 19, at $E/N = 1.5 \text{ Td}$: $\eta_{v,N_2} < 0.05$; $\eta_{v,O_2} \approx 0.65$; where η_{v,N_2} is the fraction of the Joule dissipation spent on the excitation of the N_2 vibrational mode, and η_{v,O_2} is the same for the O_2 vibrational mode. Thus, although about two thirds of the Joule dissipation goes into vibrational excitation, the Joule dissipation itself is only a small part of the energy addition rate (the upper plot in Fig. 7), which justifies disregard of vibrational excitation in the energy balance.

Calculations were also performed for air heated to $T = 2000 \text{ K}$, by postulating a model temperature profile

$$T(x) = \begin{cases} 2000 \text{ K}, & x < 3 \text{ cm}; \\ 1700 \exp(-((x-3)/1.5)^2) + 300 \text{ K}, & x \geq 3 \text{ cm}. \end{cases}$$

The temperature was uncoupled from beam and plasma equations. At this temperature and $p = 1 \text{ atm}$, the electron attachment frequency is $\nu_a \approx 4.37 \times 10^6 \text{ s}^{-1}$, and the detachment frequency is $k_d N_{O_2} \approx 1.93 \times 10^7 \text{ s}^{-1}$, so that the attachment is fully balanced by detachment, and an electron number density of $n_e \approx 10^{13} \text{ cm}^{-3}$ is achieved in air with relatively low electron beam current (Figs. 8 and 9).

Ionization and gas heating rates increase with the beam current density. Heating of the gas leads to its expansion and density reduction. This increases the beam relaxation length, so that the beam ionizes and heats the gas farther from the injection foil, burning its way through the gas. This is demonstrated in Figs. 10 and 11 for the beam with $j_b = 50 \text{ mA/cm}^2$ and $\epsilon_b = 15 \text{ keV}$. These calculations were coupled with a heat balance equation. For the short time after the start

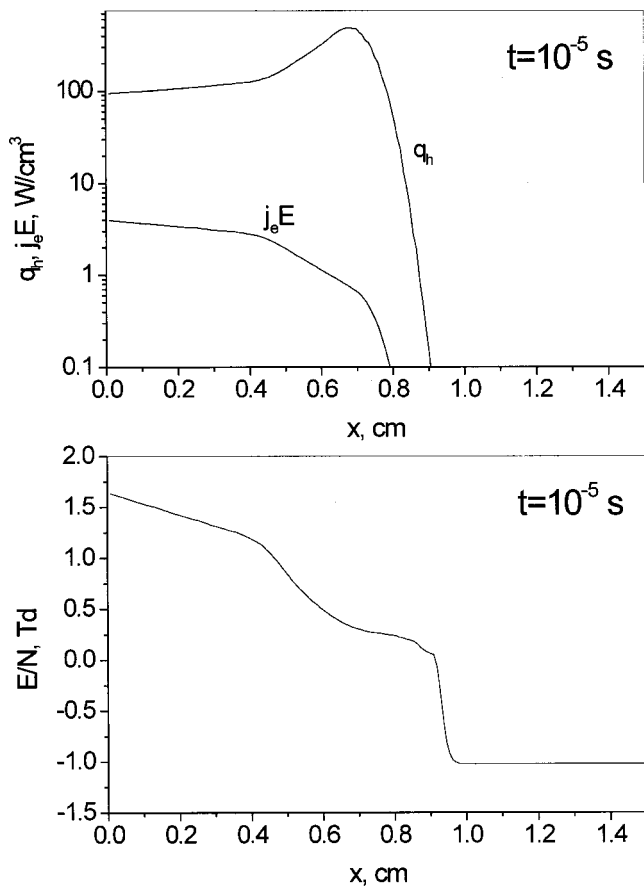


FIG. 7. Profiles of the power deposited by electron beam, q_h , Joule dissipation due to plasma electrons, $j_e E$, and the reduced electric field, E/N , at $t = 10 \mu\text{s}$ from the start of beam injection in the fountain regime in air at STP. Beam parameters are the same as in Fig. 5.

of the process, $t < 1$ ms, heat conduction losses are negligible. The characteristic time τ of the onset of natural convection can be estimated from the simple equation $g\tau^2/2 \approx h$, where h is the length scale of thermal nonuniformity, and g is the acceleration of gravity. Even with $h \approx 1$ mm, the onset of natural convection would take $\tau \sim 10$ ms. Another well known mechanism of cooling hot channels is turbulent mixing. When heating of the channel ceases, which is the case, for example, in lightning channels, cold surrounding air moves into the channels, and the fast turbulent cooling ensues. In our case, though, heating continues inside the channel, causing temperature increase and gas expansion, so that the cold surrounding gas cannot move into the channel, thus preventing the onset of turbulent cooling. Thus, the calculations at $t < 1$ ms can be done neglecting heat transfer. As seen from Fig. 10(a), by the time $t \approx 300 \mu\text{s}$ the electron density reaches 10^{13} cm^{-3} . The maximum gas temperature at this moment is $T \approx 700$ K [Fig. 10(d)]. As shown in Fig. 12, the electric field in this regime is very weak, with an E/N of less than 1.5 Td. Thus, the plasma electron temperature should be low, close to the gas temperature, and the Joule dissipation rate is much lower than the rate of beam energy losses (the upper plot in Fig. 12), thus justifying the disregard of vibrational excitation in the energy balance.

With an increasing energy of electrons in the beam, both their penetration depth and the magnitude of negative charge

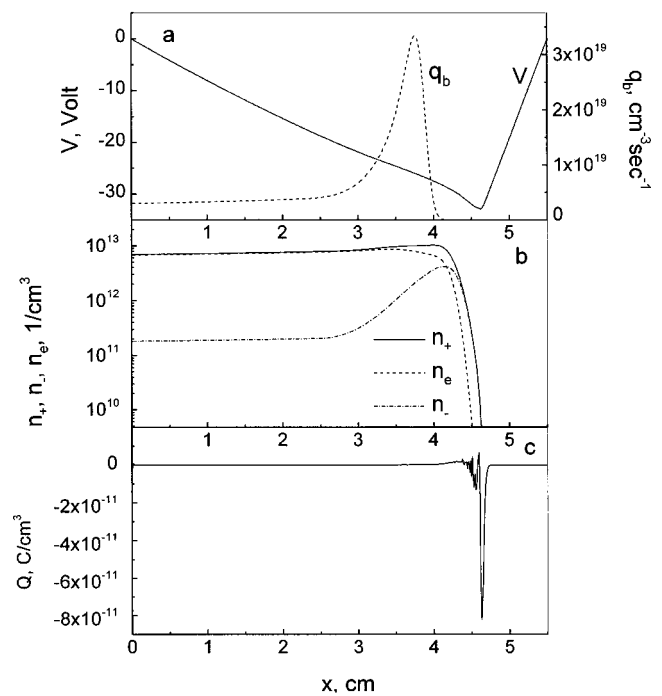


FIG. 8. Computed quasi-steady-state ($t = 20 \mu\text{s}$ from the start of beam injection) profiles of plasma parameters along the x coordinate in the fountain regime in hot air at $p = 1$ atm. The electron beam current density is 10 mA/cm^2 , and the energy of beam electrons is $\epsilon_b = 15 \text{ keV}$. (a) Electrical potential, V , and ionization rate, q_b ; (b) electron and ion number densities; (c) electric charge density, Q .

accumulated in the gas grow. However, this does not result in qualitative changes, unless the electric field in the nonionized part of the volume reaches a threshold for breakdown.

B. Thunderstorm

Suppose that a high positive voltage is applied to the anode, and the beam relaxation length is shorter than the distance to the anode. Then, even if the potential at the tip of the beam-produced plasma column were equal to that of the injection foil, the electric field between the plasma column and the anode is stronger than the field prior to beam injection.

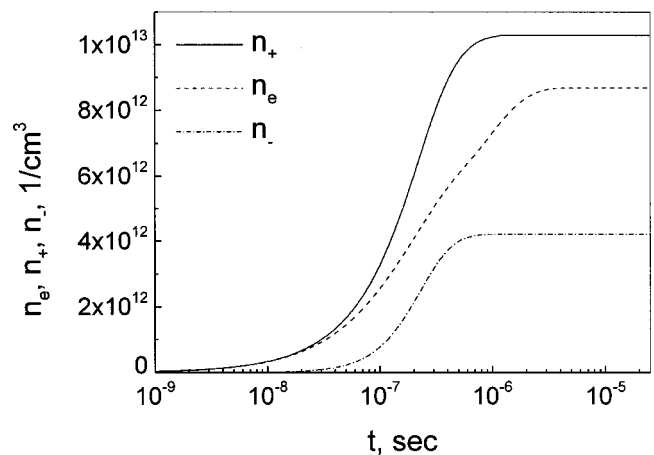


FIG. 9. Peak number densities of electrons, n_e , positive, n_+ , and negative, n_- , ions versus time from the start of beam injection in air. All parameters, including the temperature profile, are the same as in Fig. 8.

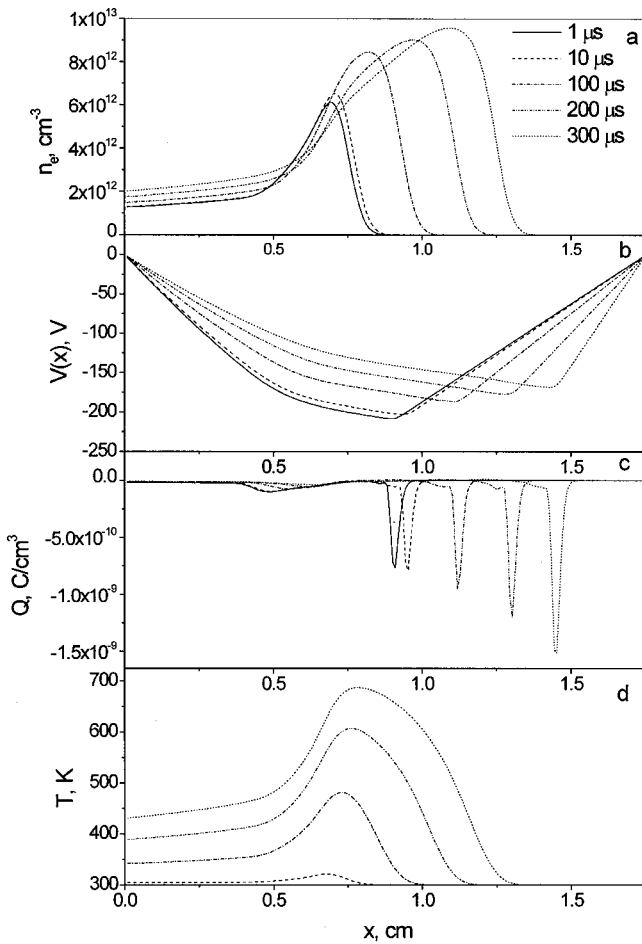


FIG. 10. The time evolution of profiles of plasma parameters in the fountain regime in air initially at STP. The electron beam current density is 50 mA/cm², and the energy of beam electrons is $\epsilon_b = 15$ keV. (a) Electron number density; (b) electric potential; (c) electric charge, Q ; (d) gas temperature.

tion. This stronger field can cause a breakdown between the tip of the plasma and the anode. Additionally, negative charge brought in by the beam distorts the distribution of electric potential, resulting in an increase of the electric field between the plasma and the anode, and increasing chances for breakdown (see Fig. 1). Whether the breakdown will be of Townsend or streamer type, depends on gas pressure and the spacing between the plasma and the anode, $d = L - l_r$. The Townsend mechanism of electric breakdown is known to occur typically at $pd < 200$ Torr·cm, while at $pd > 10^3$ Torr·cm the streamer mechanism takes over.^{17,26}

The time required to reach the breakdown field E_{br} can be estimated from the equation

$$\frac{V_a}{L - l_r} + \frac{[j_b - j_e(t)]t}{2\epsilon_0} = E_{br}. \quad (16)$$

Clearly, increasing the anode voltage V_a and making the beam relaxation length close to the distance to the anode helps the breakdown. The second term on the left-hand side of Eq. (16) is negative charge at the tip of the beam-generated plasma column. Higher beam currents shorten the time t needed to reach breakdown. The return current of

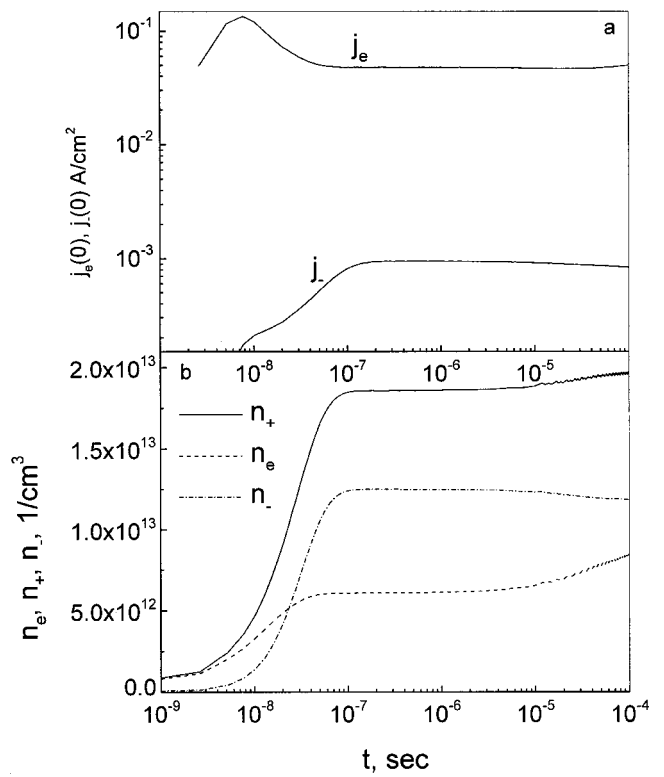


FIG. 11. (a) Back current of plasma electrons, $j_e(0)$, and negative ions, $j_-(0)$, to the foil, and (b) peak electron and positive and negative ion densities in the plasma, n_e , n_+ , and n_- , versus time from the start of beam injection in the fountain regime. The gas and electron beam parameters are the same as in Fig. 10.

plasma electrons to the cathode (foil), $j_e(t)$, slows down the accumulation of negative charge at the tip of the plasma column, and under some conditions can prevent the breakdown. In other words, if a fountain develops rapidly, a thunderstorm is prevented. In this paper, we present results of one computed thunderstorm case. A more detailed analysis, including regimes transitional between the fountain and the thunderstorm, are to be performed in the future.

An example of the thunderstorm regime is shown in Figs. 13 and 14. The calculations were done for the following set of parameters: $j_b = 50$ mA/cm², $\epsilon_b = 15$ keV; $L = 1.75$ cm, and $V(L) = 10$ kV. As seen in Fig. 13, it takes $t = 7$ ns for the electric field between the plasma and the anode to reach about 17 kV/cm, which is higher than 50% of the breakdown field in atmospheric air.¹⁷ One-dimensional modeling is certainly not adequate for an analysis of streamer development.²⁶ Indeed, the very reason for streamer breakdown in electric fields weaker than the critical breakdown field is that near the tip of the streamer the electric field is amplified because of the electrostatic polarization and the tip curvature.¹³ The curvature radius is obviously very important for the streamer initiation and growth. Leaving the task of developing a more comprehensive model of the thunderstorm for the future, we can for now use a rule of thumb that the electric field is typically amplified by a factor of 2–3 because of the curvature. Therefore, exceeding an electric field of 15 kV/cm in the 1D model, as shown in Fig. 13,

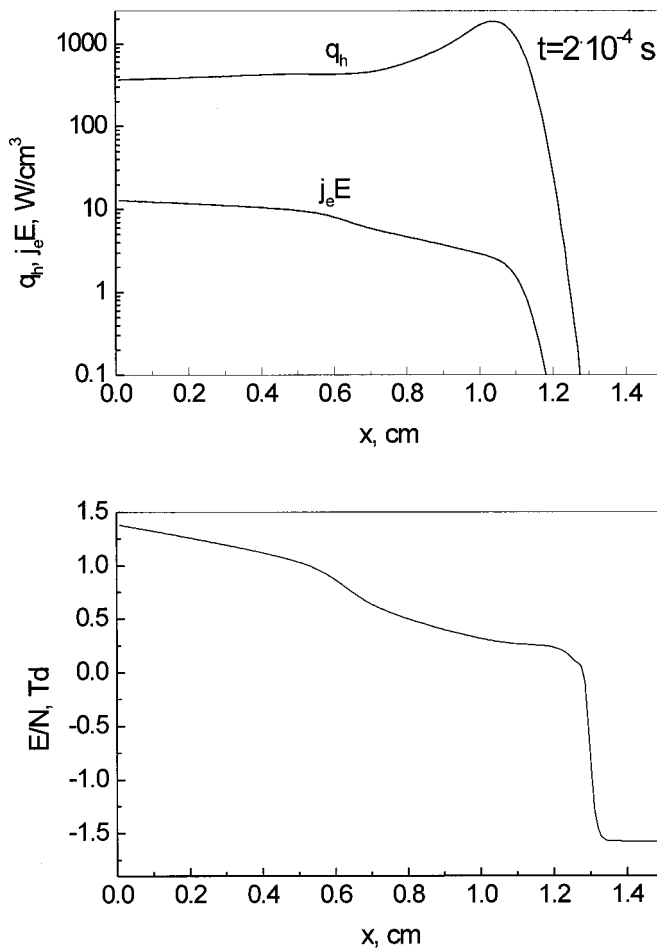


FIG. 12. The profiles of the power deposited by electron beam, q_h , Joule dissipation due to plasma electrons, $j_e E$, and the reduced electric field, E/N , at $t = 200 \mu\text{s}$ from the start of beam injection in the fountain regime in air at STP. The beam parameters are the same as in Fig. 10.

would mean that the actual field at the tip would exceed 30 kV/cm, starting a streamer.

The behavior of the return current of plasma electrons, j_e (the middle plot in Fig. 14), is explained by the evolution of electric potential and field strength (the middle and the bottom plots in Fig. 13). Initially, potential throughout the gap is higher than the potential at the injection foil, and plasma electrons drift towards the anode rather than back to the foil. As the beam brings more negative space charge, the magnitude of the negative electric field in the plasma is reduced, while the field is amplified in front of the plasma tip. However, it would take almost 9 ns for the potential anywhere inside the gap to become negative, and for the field near the foil to reverse its direction, at which moment there exists a plasma cathode inside the gap and two anodes, the foil and the original anode. As seen in Fig. 14, even at $t = 9$ ns the return current at the foil does not fully balance the beam current. Since the breakdown criterion is reached between 5 and 7 ns, the return current does not even start until the streamer onset, and in this case, $j_e = 0$ in Eq. (18). Since in this paper we only predict the onset of breakdown without modeling the subsequent dynamics of the streamer, it is difficult to say what role, if any, the return current might play in

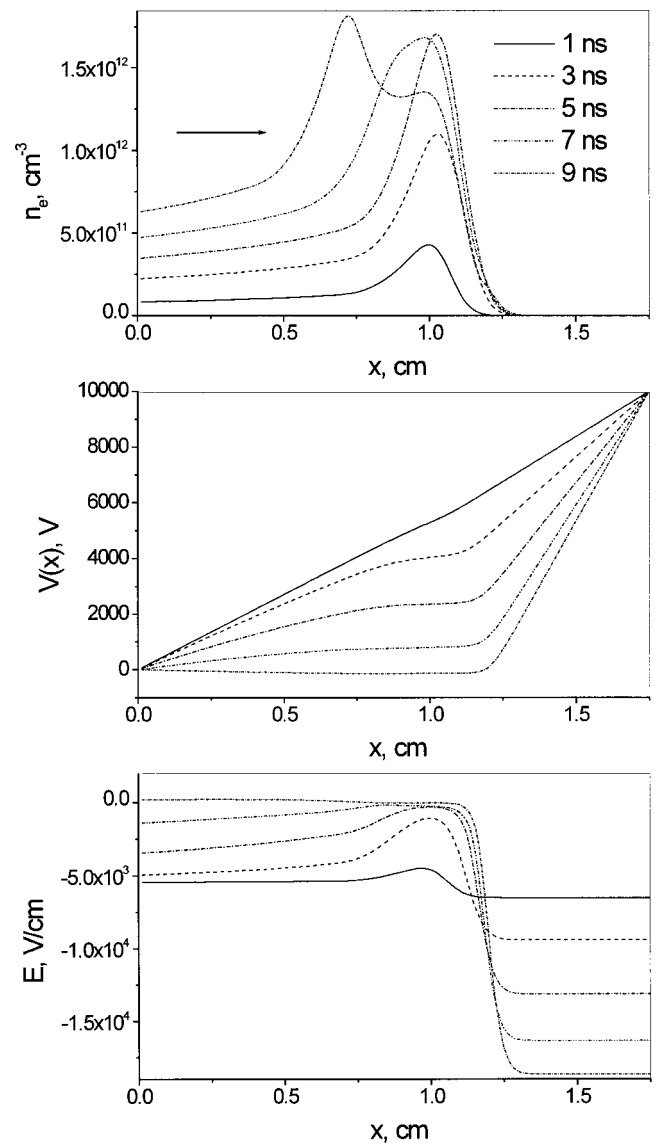


FIG. 13. The time evolution of profiles of electron number density, n_e , electric potential, $V(x)$, and electric field, E , in the thunderstorm regime in air initially at STP. The electron beam current density is 50 mA/cm^2 , and the energy of beam electrons is $\epsilon_b = 15 \text{ keV}$.

the streamer development. Also, with a set of parameters other than that in the present case, the return current could have been more significant. For example, lower initial anode voltage would have required more time to reach the breakdown field, and during that time, the electric field could have reversed its direction, thus creating the return current and affecting the breakdown criterion (18).

Note that the main requirement for electron beams injected from the cathode to the anode in high-power lasers and fast switches is to provide a uniform ionization throughout the volume. If, however, the energy of beam electrons is not high enough, so that $l_r < L$, the plasma becomes nonuniform, and electric field is distorted, resulting in some cases in sparking near the anode. This breakdown instability was experimentally observed.^{6,27} Since the instability is related to parameters of the injected beam, it has been dubbed an injection instability.^{1,6,27}

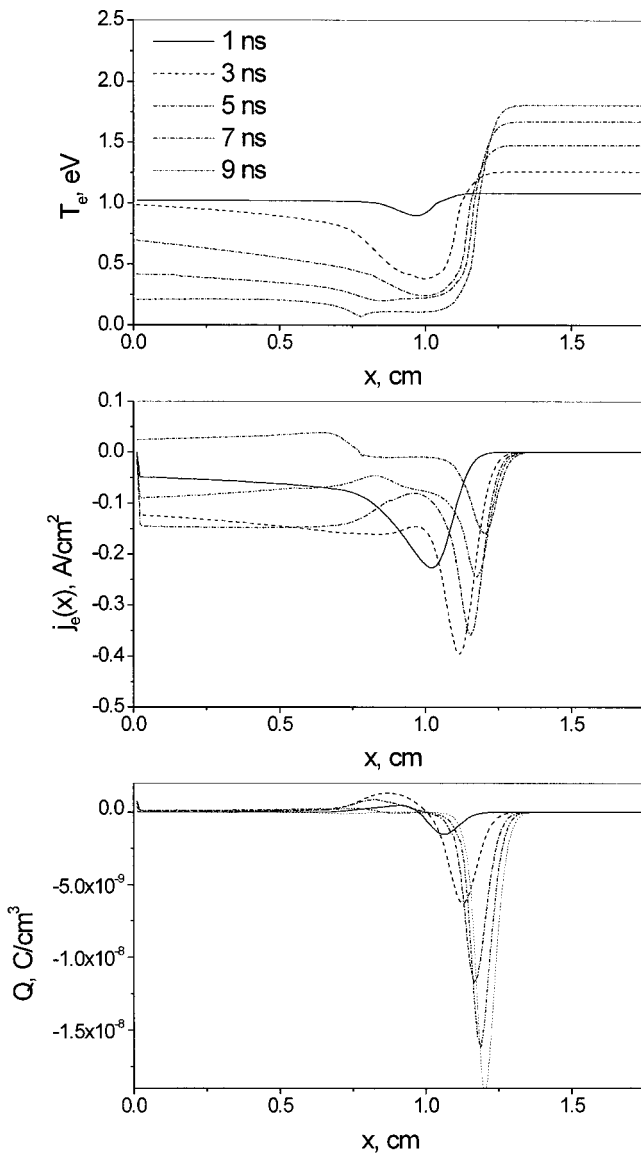


FIG. 14. The time evolution of profiles of electron temperature, T_e , current density of plasma electrons, $j_e(x)$, and space charge density, Q , in the thunderstorm regime in air initially at STP. The electron beam current density is 50 mA/cm^2 , and the energy of beam electrons is $\epsilon_b = 15 \text{ keV}$.

It is interesting to note that the electric current in the thunderstorm streamer is fully controlled by the current of the electron beam. Since the latter is, or can be made, quite low, Joule heating in the streamer can be weak, so that the streamer may not develop into a hot channel similar to lightning. In other words, a cold thunderstorm appears possible with electron beams.

IV. POWER REQUIREMENTS FOR PLASMA GENERATION

The present simplified 1D model cannot fully describe the process of establishment of steady state, including heat transfer. Nevertheless, estimates of power requirements for plasma generation and of the necessary cooling rate can be done for a given temperature and pressure.

For example, suppose that the gas temperature is maintained at $T = 2000 \text{ K}$, and that an electron beam generates a

plasma with $n_e \approx n_+ \approx 10^{13} \text{ cm}^{-3}$. If the recombination rate coefficient is about $\beta \approx 10^{-7} \text{ cm}^3/\text{s}$, then the required ionization rate is $q = \beta n_e^2 \approx 10^{19} \text{ cm}^{-3} \text{ s}^{-1}$. The power needed to sustain the ionization is then $q_h = q Y_i e \approx 55 \text{ W/cm}^3$, which also represents the gas heating rate. Since the ionization rate averaged over the beam relaxation length is $q = j_b \epsilon_b / e l_r Y_i$, and the relaxation length is inversely proportional to the gas density, $l_r \approx l_r^0 N_0 / N \approx l_r^0 T / T_0$, we find the required beam current density: $j_b \approx e q l_r^0 Y_i T / \epsilon_b T_0$. For example, for $\epsilon_b = 15 \text{ keV}$ we get $j_b \approx 23 \text{ mA/cm}^2$. These estimates agree well with the calculations depicted in Fig. 8 that show that the power required to sustain 1 cm^3 of plasma with an electron density of about 10^{13} cm^{-3} is on the order of 100 W. Increasing the energy of beam electrons moves the ionization peak farther from the injection point, but the width of the peak region does not change much, still being a few centimeters. If a wider region of high electron density is desired, one way to achieve it is to use a beam with some spread of electron energies which translates to a spread of penetration depths. Note also that the power requirement of about $50\text{--}100 \text{ W/cm}^3$ does not include a significant energy loss in the beam injection foil. In a typical metallic foil, electrons lose about $10\text{--}50 \text{ keV}$. Thus, the full cost of sustaining the plasma region with 10^{13} electrons/ cm^3 could be a few times higher than the $50\text{--}100 \text{ W/cm}^3$ required for ionization.

A temperature of 2000 K virtually eliminated electron attachment, reducing the energy cost to that needed to balance the dissociative recombination. This temperature, however, does not need to be artificially maintained by a heater, since the heating rate provided by the ionizing beam is high enough. Moreover, a substantial cooling is required to keep temperature from increasing above 2000 K. A crude estimate of the cooling requirements can be done for convective cooling where heat is removed with the flow. The effective frequency of heat removal is roughly $\nu_u = 2u/D$, where u is the gas velocity, and D is the length of the hot region. At steady state, $\rho c_p (T - T_0) \nu_u = Q_b$. From this simple formula, to sustain a temperature differential of $T - T_0 = 1700 \text{ K}$ in a 10 cm long ($D = 0.1 \text{ m}$) gas layer near the surface at the heating rate $q_h \approx 100 \text{ W/cm}^3$, flow velocity should be about 15 m/s. If the plasma length along the flow is 1 m, then a 150 m/s flow will keep the temperature from increasing above the 2000 K limit.

V. CONCLUDING REMARKS

Electron beams represent perhaps the most energy-efficient way to ionize gases at relatively low temperatures, when thermal ionization is negligible. Injecting beams of appropriate energy and current density, stable and controlled plasmas with high electron number density can be created in high-pressure gases. It turns out that dynamics of electron beam-generated plasmas, when the beam relaxation length is shorter than the distance to the anode or other metallic objects, is quite interesting. In this paper, we pointed out and analyzed two distinct regimes of beam-produced plasmas: a fountain and a thunderstorm. The two regimes differ in the way the negative space charge brought in by the beam is

removed: by the return current of plasma electrons to the injection foil (fountain) or by streamer breakdown (thunderstorm). It is interesting to note that the fountain regime is, in a sense, similar to the so-called negative glow part of glow discharge,^{5,12} where high-energy electrons arriving from the cathode sheath generate very efficient ionization, although the fountain has much larger spatial dimensions than those of negative glow at high gas density.

In our modeling, we considered an idealized one-dimensional problem. As discussed in Sec. II, a 1D analysis can be viewed as a first approximation if the beam is injected through either a very thin foil or a differentially pumped port, and if a strong magnetic field is used for guiding and confining the beam and the plasma. Additionally, our analysis was limited to beams that are originally monoenergetic. By modifying the boundary condition (5), energy spread of the injected beam can be easily accounted for.

In two and three dimensions, the dynamics of both fountain and thunderstorm discharges may be quite interesting. As was already mentioned, a thunderstorm, that is, a breakdown between the negatively charged cloud and the anode, could occur at a substantially lower anode voltage than that expected from 1D modeling. The effect is due to electric field amplification at the tip of the plasma column, similar to conventional streamers.²⁶ In principle, a streamer breakdown, or a thunderstorm, is also possible between different plasma clouds created by different electron beams, since the clouds may have different electric potentials. This breakdown will be facilitated by the photoionization of gas between the clouds.

In the fountain regime, one consequence of the non-one-dimensionality of the problem is that electric field in and around the plasma column has not only axial, but also a radial component. Plasma electrons not only drift towards the foil, but also move outside the column, making the comparison with a fountain even stronger. This electron motion decreases the electric field in the plasma. Additionally, when electrons move from the heated plasma column to cold peripheral regions, they will rapidly attach to oxygen, forming a layer of ion-ion plasma around the heated electron-ion plasma column.

The fountain regime could be subject to various oscillations and instabilities. For example, perturbations of the plasma boundary could create local curved regions where electric field amplification would be strong enough to result in streamers.

Another group of phenomena could result from the effect of electron beam burning its way through the gas, as discussed earlier in this paper. Gas heating produced by the electron beam results in a density decrease, allowing the beam to penetrate deeper. New portions of the gas are then heated, and the beam can penetrate still farther. In the case computed in this paper, portions of the gas left behind con-

tinue to be heated, preventing the surrounding cold gas from moving into the channel. If, however, the heating stops, so that the channel begins to cool, a radial flow of cold gas from the peripheral to the central regions would start. This may eventually result in turbulence generation, oscillations of the beam penetration depth and of the local ionization fraction. Phenomena as complex as these certainly call for a more sophisticated 2D or 3D model to be developed in the future.

ACKNOWLEDGMENT

This work was supported by the Director of Defense Research and Engineering "Air Plasma Ramparts" Multi-disciplinary University Research Initiative under Dr. Robert Barker of the Air Force Office of Scientific Research.

- ¹Yu. I. Bychkov, Yu. D. Korolev, and G. A. Mesyats, *Inzheksionnaia Gazovaia Elektronika* (Nauka, Novosibirsk, 1982) (Injection Gaseous Electronics, in Russian).
- ²R. B. Miller, *An Introduction to the Physics of Intense Charged Particle Beams* (Plenum, New York, 1982).
- ³D. W. Swain, *J. Appl. Phys.* **43**, 396 (1972).
- ⁴P. A. Miller and J. B. Gerardo, *J. Appl. Phys.* **43**, 3008 (1972).
- ⁵D. A. McArthur and J. W. Poukey, *Phys. Rev. Lett.* **27**, 1765 (1971).
- ⁶S. A. Genkin, Yu. D. Korolyov, G. A. Mesyats, and V. B. Ponomarev, *Pis'ma Zh. Tekh. Fiz.* **8**, 641 (1982).
- ⁷R. F. Fernsler, W. M. Manheimer, R. A. Meger, J. Mathew, D. P. Murphy, R. E. Pechacek, and J. A. Gregor, *Phys. Plasmas* **5**, 2137 (1998).
- ⁸J. Mathew, R. F. Fernsler, R. A. Meger, J. A. Gregor, D. P. Murphy, R. E. Pechacek, and W. M. Manheimer, *Phys. Rev. Lett.* **77**, 1982 (1996).
- ⁹W. M. Manheimer, *IEEE Trans. Plasma Sci.* **PS-19**, 1228 (1991).
- ¹⁰R. A. Meger, J. Mathew, J. A. Gregor, R. E. Pechacek, R. F. Fernsler, W. M. Manheimer, and A. E. Robson, *Phys. Plasmas* **2**, 2532 (1995).
- ¹¹D. R. Suhre and J. T. Verdeyen, *J. Appl. Phys.* **47**, 4484 (1976).
- ¹²V. P. Konovalov and E. E. Son, *Sov. Phys. Tech. Phys.* **25**, 178 (1980).
- ¹³G. B. Lappo, M. M. Prudnikov, and V. G. Chicherin, *High Temp.* **18**, 527 (1980).
- ¹⁴Yu. P. Raizer and M. N. Shneider, *High Temp.* **27**, 329 (1989).
- ¹⁵S. Yoshida, A. V. Phelps, and L. C. Pitchford, *Phys. Rev. A* **27**, 2858 (1983).
- ¹⁶V. P. Konovalov and E. E. Son, *Sov. Phys. Tech. Phys.* **26**, 328 (1981).
- ¹⁷Yu. P. Raizer, *Gas Discharge Physics* (Springer-Verlag, Berlin, 1991).
- ¹⁸Yu. P. Raizer and M. N. Shneider, *High Temp.* **29**, 833 (1991).
- ¹⁹N. L. Alexandrov, F. I. Vysikailo, R. Sh. Islamov, I. V. Kochetov, A. P. Napartovich, and V. G. Pevgov, *High Temp.* **19**, 17 (1981).
- ²⁰J. M. Anderson, *J. Appl. Phys.* **31**, 511 (1960).
- ²¹S. O. Macheret, M. N. Shneider, R. B. Miles, R. J. Lipinski, and G. L. Nelson, Paper AIAA-98-2922 (American Institute of Aeronautics and Astronautics, Washington, DC, 1998).
- ²²Y. Itikawa, M. Hayashi, A. Ichimura, K. Onda, K. Sakimoto, K. Takayanagi, M. Nakamura, H. Nishimura, and T. Takayanagi, *J. Phys. Chem. Ref. Data* **15**, 985 (1986).
- ²³Y. Itikawa, M. Hayashi, A. Ichimura, K. Onda, K. Sakimoto, K. Takayanagi, Y. Hatano, M. Hayashi, H. Nishimura, and S. Tsurubuchi, *J. Phys. Chem. Ref. Data* **18**, 23 (1989).
- ²⁴Y. Itikawa, "Electron collisions with N₂, O₂, and O: What we do and do not know," ISAS Research Note 526, 1993.
- ²⁵I. A. Kossyi, A. Yu. Kostinsky, A. A. Matveyev, and V. P. Silakov, *Plasma Sources Sci. Technol.* **1**, 207 (1992).
- ²⁶E. M. Bazelyan and Yu. P. Raizer, *Spark Discharge* (CRC Press, Boca Raton, FL, 1997).
- ²⁷G. A. Mesyats, *Sov. Tech. Phys. Lett.* **1**, 292 (1975).